Finite Element Analysis Methodology for Additive Manufactured Tooling Components

Nilesh Warad, Janardhan Rao, Kedar Kulkarni, Avinash Dandekar, Manoj Salgar, and Malhar Kulkarni

***Abstract*—Fused deposition modeling (FDM) for additive manufacturing is constantly growing as an innovative process across the industry in areas of prototyping, tooling, and production parts across most manufacturing industry verticals such as Aerospace, Automotive, Agricultural, Healthcare, etc. One such application that is widely used is for tooling on the shop floor e.g. for pick-off tools, assembly fixtures etc. For tooling applications printing the solid fill component with +45/-45 raster is common practice. There is a requirement for finite element analysis to validate the strength of 3D printed components for some specific applications in tooling, but due to the anisotropic behavior of 3D printed parts and the unavailability of all mechanical properties FE analysis of 3D printed parts is sometimes challenging. Advance approaches like multiscale modeling approach requires specialized & costly analytical tools. So, to understand the behavior of additively manufactured parts the team has conducted a few tests and compared the results. In this work, solid-filled dog-bone tensile test and three-point bending test specimens were printed with +45/-45 raster orientation and tested in the lab. Tensile test specimens were built with flat, on-edge, and up-right orientations and tested to determine the directional properties of young's modulus. Using mechanical properties from the tension test 3 points bending test is simulated in FE software-ANSYS. The FE modeling was done in two ways, in first model orthotropic properties were assigned to the specimen, and for second model isotropic properties were assigned. For isotropic modeling least value of young's modulus is used. Simulation results of three-point bending test shows that in the linear region of force-deflection curve, deformation values from FE model with both orthotropic and isotropic modeling are in good agreement with the experimental results. Also, the difference in stress results between isotropic and orthotropic FE model is almost negligible. To support this observation, study is performed for various conditions. The specimens were printed with ABS material on Ultimaker® and ASA material on Stratasys® Fortus 360mc™ machine with T12, T16 and T20 nozzle settings. Study shows, for tooling applications if the 3D printed solid-filled components are designed with a certain factor of safety then validating its strength with isotropic material properties will give acceptable results. The advantage of this approach is getting the isotropic mechanical properties is easy and modeling with FE modeling will be simple.**

***Index Terms*—3D-printing, additive manufacturing, mechanical properties of materials, Finite Element Analysis (FEA).**

Manuscript received June 29, 2022; revised October 21, 2022.

The authors are with John Deere India Pvt Ltd., India (email: WaradNilesh@johndeere.com, sammetajanardhanrao@johndeere.com, kulkarnikedar@johndeere.com, dandekaravinash@johndeere.com, salgarmanojkumar@johndeere.com, kulkarnimalharms@johndeere.com)

I. Introduction

FDM is the most common techniques used for 3D printers and has become one of the most popular rapid prototyping techniques in the last decade. It involves the melting and extrusion of a filament material at specific intervals and predetermined locations where it cools and solidifies, one layer at a time. Because of rapid prototyping 3D printing is finding wide application in tooling on the shop floor. Finite Element Analysis (FEA) helps validate the strength of 3D printed components for specific applications. Due to the layer-by-layer building mechanism, part orientation plays a significant role in the mechanical properties, dimensional accuracy, and surface finish. In addition, other building parameters in FDM, such as raster angle, also contribute to the anisotropic material properties [1]. Several research on the elastic properties have been carried out on many FDM-printed polymer materials such as Acrylonitrile Butadiene Styrene (ABS) [2], polycarbonate (PC) [3]. However, to get full orthotropic properties of 3D-printed materials, various mechanical testing needs to be performed. Cost and time involved in these testing is considerable. Hence, we find limited usage of designing of 3-D printed structural components using computer simulation. For tooling applications printing the solid fill component with +45/-45 raster is common practice. In this work, to deduce the elastic constants of the 3D printed material, solid filled dog-bone tensile test and three-point bending test specimens were printed with +45/-45 raster orientation and tested in the lab. Dog-bone specimen were tested to determine the directional properties of Young's modulus properties. Using mechanical properties from the tension test we have simulated 3 points bending test in FE software-ANSYS. The FE modelling was done in two ways, in first model orthotropic properties to the specimen were assigned, and for second model isotropic properties were assigned. For isotropic modelling least value of Young's modulus is used. Simulation results shows that in linear region, deformation values from FE model with both orthotropic and isotropic modelling are in good shown agreement with the experimental results. Also difference in stresses results between FE model orthotropic and isotropic models is almost negligible. To support this observation, study is performed for various conditions. Study had shown, if we design solid filled 3D printed components with certain factor of safety then validating the strength of the component with isotropic material properties will give acceptable results. The advantage of this approach is modelling with isotropic material properties is simple to use of mechanical properties is easily available.

DOI: 10.7763/IJET.2022.V14.1202

II. Theory

The strain–stress relationships of an orthotropic material can be written in terms of a compliance matrix C_{ij}

$$\varepsilon_i = S_{ij}\sigma_j$$

where $\varepsilon_i = \begin{bmatrix}\varepsilon_x & \varepsilon_y & \varepsilon_z & \gamma_{yz} & \gamma_{xz} & \varepsilon_{xy}\end{bmatrix}^T$ is strain and $\sigma_j = \begin{bmatrix}\sigma_x & \sigma_y & \sigma_z & \tau_{yz} & \tau_{xz} & \tau_{xy}\end{bmatrix}^T$ is stress.

From the symmetry of the compliance matrix

$$S_{ij} = \begin{bmatrix} S_{11} & S_{12} & S_{13} & 0 & 0 & 0 \\ S_{12} & S_{22} & S_{23} & 0 & 0 & 0 \\ S_{13} & S_{23} & S_{33} & 0 & 0 & 0 \\ 0 & 0 & 0 & S_{44} & 0 & 0 \\ 0 & 0 & 0 & 0 & S_{55} & 0 \\ 0 & 0 & 0 & 0 & 0 & S_{66} \end{bmatrix}$$

$$S_{ij} = \begin{bmatrix} \frac{1}{E_1} & \frac{-\mu_{21}}{E_2} & \frac{-\mu_{31}}{E_3} & 0 & 0 & 0 \\ \frac{-\mu_{12}}{E_1} & \frac{1}{E_2} & \frac{-\mu_{32}}{E_3} & 0 & 0 & 0 \\ \frac{-\mu_{13}}{E_1} & \frac{-\mu_{23}}{E_2} & \frac{1}{E_3} & 0 & 0 & 0 \\ 0 & 0 & 0 & \frac{1}{G_{23}} & 0 & 0 \\ 0 & 0 & 0 & 0 & \frac{1}{G_{31}} & 0 \\ 0 & 0 & 0 & 0 & 0 & \frac{1}{G_{12}} \end{bmatrix}$$

$$\frac{\mu_{21}}{E_2} = \frac{\mu_{12}}{E_1}, \quad \frac{\mu_{31}}{E_3} = \frac{\mu_{13}}{E_1} \text{ and } \frac{\mu_{32}}{E_3} = \frac{\mu_{23}}{E_2}$$

Hence to model 3D printed the orthotropic behavior of the 3D printed part in FE software we need 9 independent material constants. The constants are needed to derive from the lab tests of the standard specimens.

III. Specimen Design and Fabrication

A. Specimen Design

Materials tested in this study were ASA and ABS. ASA samples were printed on Stratasys® Fortus 360mc™ 3D-printer and ABS samples were built on Ultimaker® 2 3D-printer. On Stratasys® 3D-printer ASA samples were printed with two different nozzle settings with T16 model tip and other with T20 model tip. The specimen geometries for tension test followed specifications outlined in ASTM D-638 for the Type IV tensile specimens. Specimen dimensions are shown in Fig. 1 with thickness of 4mm.

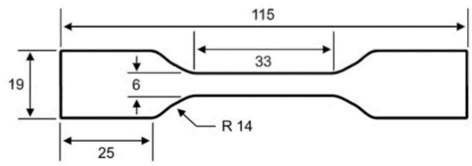

Fig. 1. Schematic representation of ASTM D638 Type IV tensile specimen with relevant dimensions in mm.

The entire list of machine parameters set for building ASA and ABS samples are listed in Table I. The raster orientation selected was [+45/-45]. This raster orientations were selected as majority of 3D-printers using an alternating raster pattern as the default printing scheme.

TABLE I: 3D-Printing Process Settings for the Stratasys® Fortus and Ultimaker®

Parameters	Stratasys® Fortus 450 mc ASA Material		Ultimaker® 2 machine ABS Material
	T16 Nozzle	T20 Nozzle	
Air gap (mm)	0.0	0.0	0.0
Slice height (mm)	0.1	0.1	0.1
Extrusion width (mm)	0.4	0.4	0.4
Nozzle size (mm)	0.4	0.4	0.4
Fill (%)	100	100	100

Tensile test samples were built in three orientations. These orientations are based upon which plane the front face of the specimen resides and were named accordingly. The three orientations investigated were flat (XY plane), on-edge (XZ plane), and up-right (ZX plane) and for clarification purposes are illustrated in Fig. 2 along with the raster orientation.

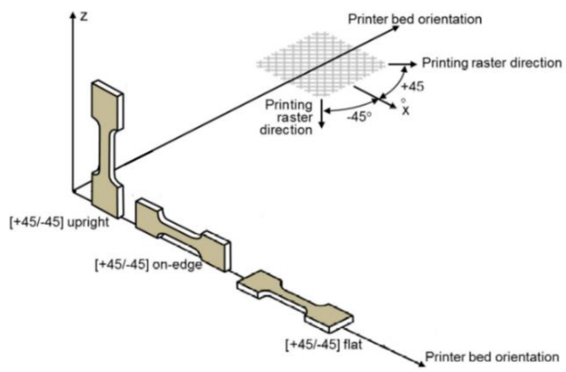

Fig. 2. Graphic representation of the printer bed orientations (flat, on-edge, and up-right) [4].

IV. Test Results

A. Tensile Test Results with ASA Samples

On Stratasys® 3D-printer ASA samples were printed with two different machine settings one with T16 model tip and other with T20 model tip. The tension specimens were tested in batches of five printed for each orientation and the results for all five tests averaged to find the mechanical properties. Results reported from tension tests are Young's modulus, Tensile Strength, and strain at failure. Fig. 3 shows stress-strain curve graphs for the each of the tests performed of T16 nozzle setting samples. Similar graph we got for T20 nozzle setting samples as well (which are not shown here because of space constrain). Mechanical properties derived from the tension tests are listed in Table II.

TABLE II: Tensile Test Properties for ASA Specimens

	T16 Nozzle Orientation			T20 Nozzle Orientation		
Property	[+45/-45] Flat (X)	[+45/-45] on-edge (Y)	[+45/-45] up-right (Z)	[+45/-45] Flat (X)	[+45/-45] on-edge (Y)	[+45/-45] up-right (Z)

Young's Modulus (MPa)	1746	1668	1666	1890	1743	1668
Ultimate Strength (MPa)	25.66	25.42	18.94	29.26	29.16	17.76
Strain at Failure (%)	6.34	8.39	1.50	5.80	5.83	1.33

These mechanical properties will further be used in performing 3-point bending test simulation

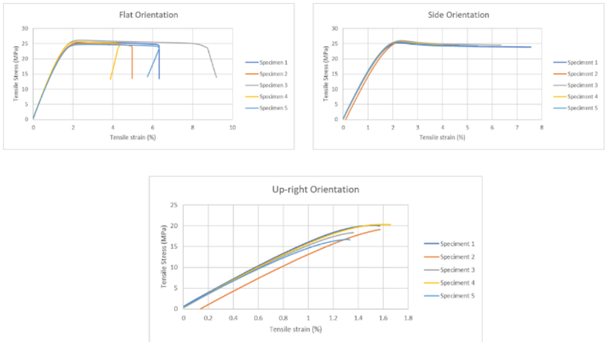

Fig. 3. Stress-strain curve for ASA samples with T16 nozzle.

TABLE III: TENSILE TEST PROPERTIES FOR ABS SPECIMENS [4]

Property	Orientation		
	[+45/-45] Flat (X)	[+45/-45] on-edge (Y)	[+45/-45] up-right (Z)
Young's Modulus (MPa)	2040	2020	1960
Ultimate Strength (MPa)	30.3	30.0	29.9
Strain at Failure (%)	8.89	5.41	1.84

B. Tensile Test Results with ABS Samples

ABS samples were built on an Ultimaker® 2 3D-printer. The tension specimens were tested in batches of five printed for each orientation and the results for all five tests averaged to find the mechanical properties. From the tensile tests we were expected to get results for Young's modulus, Tensile Strength, Strain at failure. However, because of limitation of lab test set up appropriate data for the Young's modulus was not collected. For this reason, we have compared the ultimate strength data from the actual test and literature [4]. While doing this it is ensured that the 3D printer machine parameters for lab test samples and literature data samples are same. Ultimate tensile strength values from the lab test are 32.2 MPa, 30.9 MPa and 28.1 MPa for flat, on-edge and up-right orientation, respectively. Since these ultimate strength values are matching closely with literature data [3], mechanical properties for ABS sample are referred from the literature. Table III enlists the results mechanical properties from tension test for ABS samples.

V. FINITE ELEMENT SIMULATION OF 3-POINT BENDING TEST

Using mechanical properties from the tension test we have simulated three-points bending test in FE software-ANSYS. Specimen dimensions and test fixture dimensions for three point bending test are shown in Fig. 4.

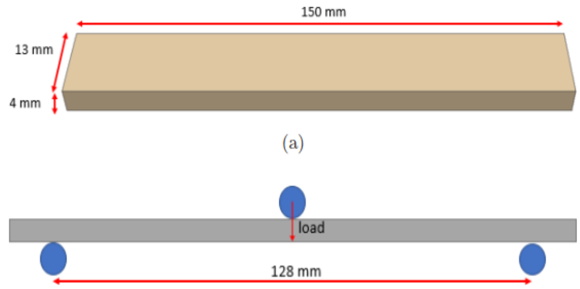

Fig. 4. Schematic representation of Three-point bending test specimen [5].

The FE simulation of three point bending test modelling was done in two ways, in first model orthotropic material properties were assigned, and for second model isotropic properties were assigned. For isotropic modelling least value of Young's modulus is used which is observed with up-right orientation.

A. Results for ASA Samples with T16 Nozzle

For three-point bending test five samples with ASA material were printed all with flat orientation and in 45◦/−45◦ raster configuration. Fig. 5 shows deformation and stress plots from the FE simulation results with orthotropic and isotropic material assignment along with mechanical properties used in FE model. Here Young's modulus values are referred from actual tensile tests as explained in previous section whereas Poisson's ratio and shear modulus data is referred from literature [5].

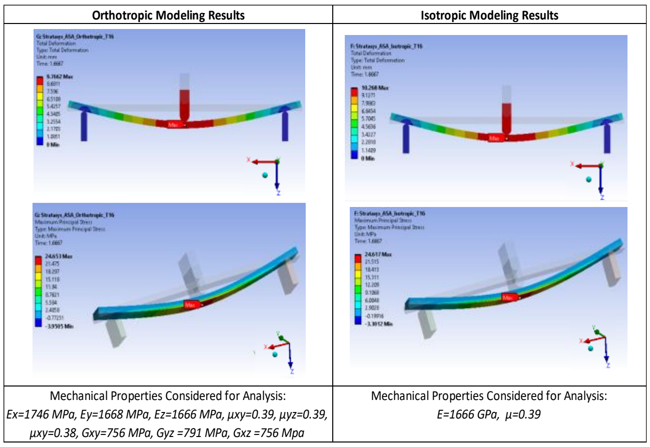

Fig. 5. Deformation and stress results from FE model for ASA sample printed with T16 nozzle.

Simulation and experimental results are compared using the force–deflection relations in Fig. 6. Table IV shows the percentage difference in deflection results from FE model with lab test results. It is observed that in the linear region of force-deflection curve, deformation results from FE model with both approaches shows good correlation with lab test results. The percentage difference between the deflection results from orthotropic and isotropic model is only 5%. Table V shows the comparison of the principal stress results with isotropic and orthotropic models, which shows that the principal stress results with both the approaches are matching within 1%.

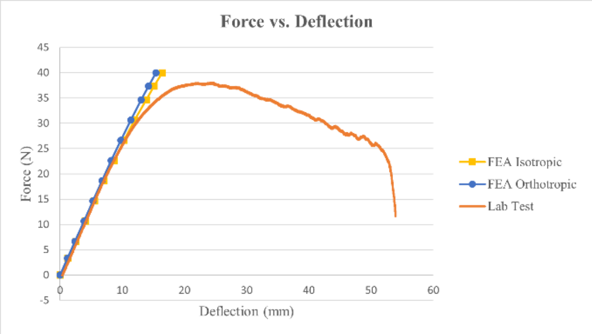

Fig. 6. Force–displacement responses comparison of T16 ASA specimens for three-point bending.

TABLE IV: COMPARISON DEFLECTION RESULTS FOR T16 SPECIMEN ASA

Load (N)	Lab Test Deflection (mm)	FEA Isotropic Deflection (mm)	FEA Orthotropic Deflection (mm)	Diff between FE results
3.3	1.5	1.26	1.19	5%
6.7	2.7	2.53	2.4	5%
10.7	4.13	4.04	3.84	5%
14.7	5.52	5.55	5.28	5%
18.7	7.01	7.08	6.72	5%
22.7	8.62	8.64	8.21	5%
26.7	10.41	10.26	9.76	5%

TABLE V: COMPARISON PRINCIPAL STRESS RESULTS FOR T16 SPECIMEN ASA

Load (N)	FEA Isotropic Stress (MPa)	FEA Orthotropic Stress (MPa)	Diff between FE results
3.3	3.06	3.07	-0.1%
6.7	6.15	6.15	-0.1%
10.7	9.82	9.84	-0.2%
14.7	13.47	13.49	-0.1%
18.7	17.14	17.13	0.0%
22.7	20.85	20.85	0.0%
26.7	24.62	24.65	-0.1%

B. *For ASA Samples with T20 Nozzle*

For three-point bending test five samples with ASA material were printed all with flat orientation and in 45∘/−45∘ raster configuration. Fig. 7 shows deformation and stress plots from the FE simulation results with orthotropic and isotropic material assignment along with mechanical properties used in FE model. Here Young's modulus values are referred from actual tensile tests as explained in previous section whereas Poisson's ratio and shear modulus data is referred from literature [5].

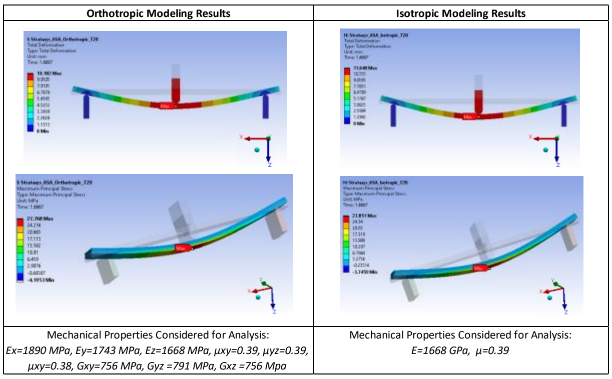

Fig. 7. Deformation and stress results from FE model for ASA sample printed with T20 Nozzle.

Simulation and experimental results are compared using the force–deflection relations in Fig. 8. Table VI shows the percentage difference in deflection results from FE model with lab test results. It is observed that in the linear region of force-deflection curve, deformation values from FE model with both approaches are similar with that of lab test results. The percentage difference between the deflection results from orthotropic and isotropic model is only 14%. However, percentage difference between principal stress results with isotropic and orthotropic models is within 1% as shown in Table VII.

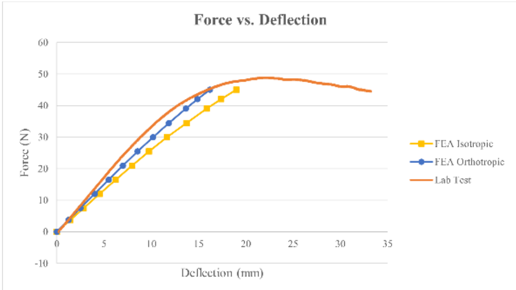

Fig. 8. Force–displacement responses comparison of T20 ASA specimens for three-point bending.

TABLE VI: COMPARISON DEFLECTION RESULTS FOR T20 SPECIMEN ASA

Load (N)	Lab Test Deflection (mm)	FEA Isotropic Deflection (mm)	FEA Orthotropic Deflection (mm)	Diff between FE results
3.7	1.2	1.41	1.24	14%
7.5	2.25	2.84	2.5	14%
12.0	3.5	4.53	3.99	13%
16.5	4.76	6.23	5.49	14%
21.0	6.02	7.97	7.00	14%
25.5	7.38	9.76	8.55	14%
30.0	8.83	11.64	10.18	14%

TABLE VII: COMPARISON PRINCIPAL STRESS RESULTS FOR T20 SPECIMEN ASA

Load (N)	FEA Isotropic Stress (MPa)	FEA Orthotropic Stress (MPa)	Diff between FE results
3.7	3.45	3.45	-0.1%
7.5	6.92	6.93	0.0%
12.0	11.04	11.07	-0.3%
16.5	15.14	15.17	-0.2%
21.0	19.30	19.28	0.1%
25.5	23.51	23.48	0.1%
30.0	27.85	27.77	0.3%

C. *For ASA Samples with T12 Nozzle*

For this study actual lab test were not performed and material data is referred from the literature [5]. Fig. 9 shows deformation and stress plots from the FE simulation results with orthotropic and isotropic material assignment along with mechanical properties used in FE model. Here all mechanical properties data is referred from literature.

Simulation and experimental results are compared using the force–deflection relations in Fig. 10. Table VIII shows the percentage difference in deflection results from FE model with lab test results. It is observed that in the linear region of force-deflection curve, deformation values from FE model with both approaches are similar with that of lab test results. The percentage difference between the deflection results from orthotropic and isotropic model is only 11%. However, percentage difference between principal stress results with isotropic and orthotropic models is within 1% as shown in Table IX.

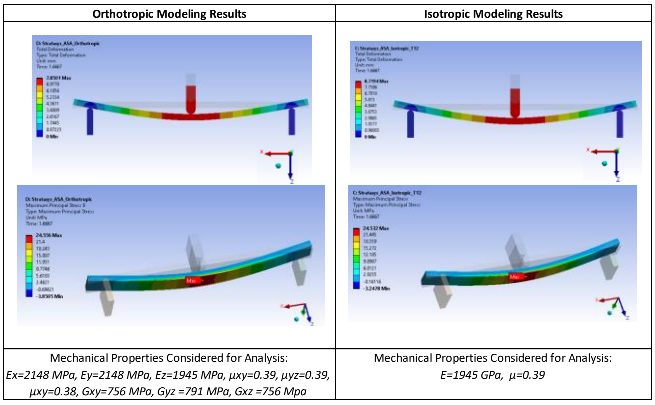

Fig. 9. Deformation and stress results from FE model for T12 ASA sample.

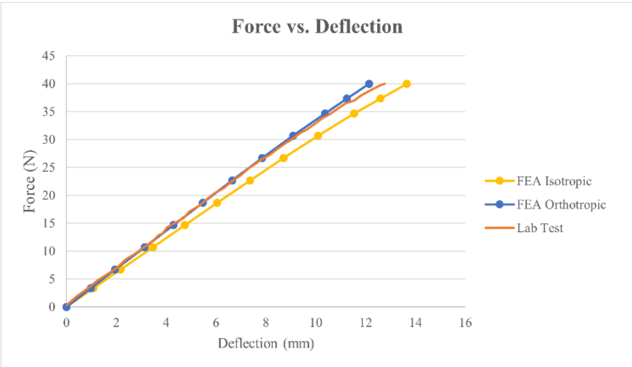

Fig. 10. Force–displacement responses comparison of T12 ASA specimens for three-point bending.

TABLE VIII: COMPARISON DEFLECTION RESULTS FOR T12 SPECIMEN ASA

Load (N)	Lab Test Deflection (mm)	FEA Isotropic Deflection (mm)	FEA Orthotropic Deflection (mm)	Diff between FE results
3.3	0.89	1.08	0.97	11%
6.7	1.93	2.16	1.95	11%
10.7	3.02	3.47	3.13	11%
14.7	4.2	4.76	4.29	11%
18.7	5.5	6.05	5.47	11%
22.7	6.68	7.37	6.64	11%
26.7	7.9	8.72	7.85	11%

TABLE IX: COMPARISON PRINCIPAL STRESS RESULTS FOR T12 SPECIMEN ASA

Load (N)	FEA Isotropic Stress (MPa)	FEA Orthotropic Stress (MPa)	Diff between FE results
3.3	3.06	3.06	0.0%
6.7	6.14	6.15	-0.1%
10.7	9.85	9.87	-0.2%
14.7	13.48	13.53	-0.3%
18.7	17.13	17.87	-4.1%
22.7	20.81	20.84	-0.1%
26.7	24.53	24.55	-0.1%

D. For ABS Samples

For three point bending test five samples with ABS material were printed with flat orientation and in $45^\circ/-45^\circ$ raster configuration. Fig. 11 shows deformation and stress plots from the FE simulation results with orthotropic and isotropic material assignment along with mechanical properties used in FE model. Here all mechanical properties data is referred from literature.

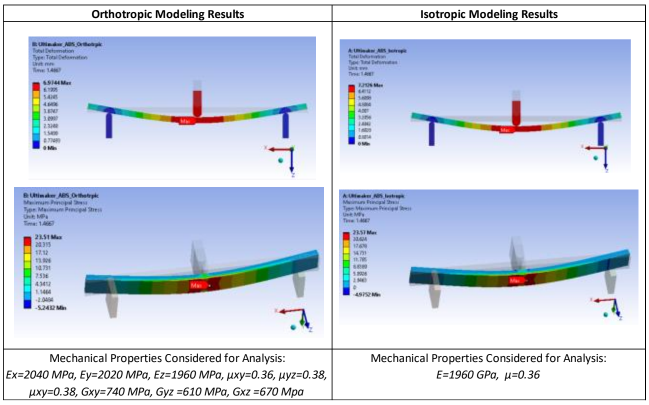

Fig. 11. Deformation and stress results from FE model for ABS samples.

Simulation and experimental results are compared using the force–deflection relations in Fig. 12. Table X shows the percentage difference in deflection results from FE model with lab test results. It is ` that in the linear region of force-deflection curve, deformation values from FE model with both approaches are similar with that of lab test results. The percentage difference between the deflection results from orthotropic and isotropic model is 4%. However, percentage difference between principal stress results with isotropic and orthotropic models is within 1% as shown in Table XI.

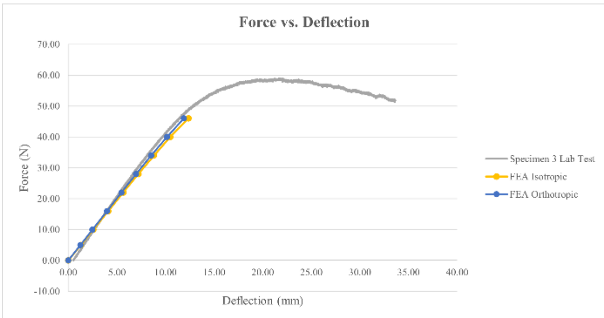

Fig. 12. Force–displacement responses comparison of ABS specimens for three-point bending.

TABLE X: COMPARISON DEFLECTION RESULTS FOR ABS SPECIMEN

Load (N)	Lab Test Deflection (mm)	FEA Isotropic Deflection (mm)	FEA Orthotropic Deflection (mm)	Diff between FE results
5.0	1.5	1.28	1.24	4%
10.0	2.7	2.58	2.49	4%
16.0	4.0	4.11	3.98	3%
22.0	5.3	5.65	5.47	3%
28.0	6.7	7.21	6.97	3%
34.0	8.2	8.81	8.53	3%
40.0	9.7	10.48	10.16	3%

TABLE XI: COMPARISON PRINCIPAL STRESS RESULTS FOR ABS SPECIMEN

Load (N)	FEA Isotropic Stress (MPa)	FEA Orthotropic Stress (MPa)	Diff between FE results
5.0	4.28	4.22	1.4%
10.0	8.51	8.45	0.7%
16.0	13.53	13.50	0.2%

22.0	18.52	18.49	0.2%
28.0	23.57	23.51	0.3%
34.0	28.66	28.62	0.1%
40.0	33.84	33.83	0.0%

VI. Conclusion and Summery

3 Point bending test of ABS samples shows, results for deflection and stress with isotropic and orthotropic material properties are closely matching and are in good agreement with test results. For ASA Samples we observe that T12 and T16 nozzle setting samples shows good correlation compared to T20 nozzle setting samples. Also, one more thing we observe here is that the mechanical properties of T20 nozzle setting samples are better than T16 samples.

To summaries study, we suggest that for the tooling component where we generally design the component with certain factor of safety, FE modeling with least isotropic material properties (Z-direction) can give fairly the acceptable results. The proposed approach in this paper is more efficient & requires less input data than detailed approach. However, it still provides good level of correlation with detailed approach. Similar study can be performed on other material like Nylon and to check the same approach is applicable.

Important consideration

- Samples considered for this study are ABS and ASA samples: with +/-45 printing orientation and solid filling
- Only pure bending load case is considered here hence the conclusion made from this study are applicable only for bending or tensile load.
- For complex loading conclusions made in this study may not be valid
- For Ultimaker® machines where parts are exposed to environment while printing, mechanical properties may vary from sample to samples

Conflict of Interest

All authors declare no conflict of interest.

Author Contributions

Nilesh Warad conducted literature survey, lab tests, and analyzed the test data. Janardhan Rao, Kedar Kulkarni and Avinash Dandekar provided the technical guidance. Nilesh Warad, Manojkumar Salgar and Malhar Kulkarni wrote the paper. All authors had approved the final version.

References

[1] M. Baumers, P. Dickens, C. Tuck, and R. Hague, "The cost of additive manufacturing: Machine productivity, economies of scale and technology-push," *Technol. Forecast. Soc. Change*, vol. 102, pp. 193-201, 2016.

[2] M. Dawoud, I. Taha, and S. J. Ebeid, "Mechanical behaviour of ABS: An experimental study using FDM and injection moulding techniques," J. Manuf. Process. 21, 39-45, 2016.

[3] J. T. Cantrell, S. Rohde, D. Damiani, R. Gurnani, L. DiSandro, J. Anton, and P. G. Ifju, "Experimental characterization of the mechanical properties of 3D-printed ABS and polycarbonate parts," *Rapid Prototyping J.*, vol. 23, pp. 811–824, 2017.

[4] J. Cantrell, S. Rohde, and D. Damiani, "Experimental characterization of the mechanical properties of 3D printed ABS and polycarbonate parts," *J. Advancement of Optical Methods in Experimental Mechanics*, vol. 3, pp. 89-105, 2016.

[5] Y. L. Yap, W. Toh, R. Koneru, and Z. Y. Chua, "Finite element analysis of 3D-Printed Acrylonitrile Styrene Acrylate (ASA) with ultrasonic material characterization," *J. Computational Materials Science and Engineering*, vol. 8, 2019.

Nilesh Warad has completed master of technology (mechanical design) in the year 2012 and bachelor of engineering (mechanical engineering) in the year 2009. He has around 10 years of experience in structural analysis using FEA. He has been working with John Deere India Pvt. Ltd. since 2018. With his current position as a lead engineer, his focus areas are tool design and structural analysis.

Janardhan Rao has master degree in tool design from Central Institute of Tool Design, Hyderabad, India. He has total of 24 years of experience in area of tool fixture design and additive manufacturing. He is currently employed with John Deere India Pvt. Ltd. as staff manufacturing engineer. He is responsible for additive manufacturing operations, new methods & applications development & new technology implementation in the area of tooling.

Kedar Kulkarni has completed master of engineering (mechanical) with design as specialization in 2005. Mr. Kedar Kulkarni has around 18 years of experience in structural analysis using FEA. He has diverse experience in product development in the sector of defense, nuclear, aerospace, agriculture. He has been working with John Deere India Pvt. Ltd. since 2008. With his current position as senior lead engineer, his focus areas are polymer mechanics, material simulation, advanced material, and light weighting.

Avinash Dandekar has completed master of engineering with tool design as specialization in 2006. Mr. Avinash Dandekar has 20 years of experience in tool design & manufacturing domain. He is associated with John Deere India Pvt Ltd. since 2008. In his current role he is responsible for tool design projects for new product development programs. His areas of interest are additive tooling, light weight tooling, and data analysis

Manojkumar Salgarhas completed his masters from National Institute of Technology, Rourkela (NITR) in 2013 and bachelors of engineering in mechanical engineering in 2010. He has published 6 papers in areas like AFM, EDM, etc. Mr. Manoj has experience of assistant professor and currently working as CAE Analysis at John Deere India Pvt. Ltd. Pune since 2019.

Malhar Kulkarni was born in Nagpur in the year 1990, has completed his master of engineering (tool design) in the year 2013 and bachelor of engineering (production engineering) in the year 2011. Mr. Kulkarni has a rich experience from the fields of aerospace and automotive industry and currently located at Pune as a lead engineer with John Deere India Pvt. Ltd.